JOURNAL OF PROPULSION AND POWER
Vol. 22, No. 6, November–December 2006

Performance of a Scramjet Combustor with Combined Normal and Tangential Fuel Injection

Scott A. Rowan* and Allan Paull†
The University of Queensland, Brisbane, Queensland 4072, Australia

The performance of a scramjet combustor with combined normal and tangential injection was experimentally investigated. Experiments were performed on a 500-mm cylindrical scramjet combustor at a freestream Mach number of 4.5, a nozzle supply pressure of 35.8 MPa, and a nozzle supply enthalpy of 5.8 MJ/kg. Hydrogen fuel was injected normally through portholes to promote combustion and tangentially through a slot to reduce viscous drag. A series of fuel injectors were used to vary the proportion of tangential to normal fuel between 45 and 100%. Reductions in the viscous drag of up to 25% were observed with the greatest reductions occurring at the lowest total equivalence ratio tested for each injector. However, the average pressure produced by combustion with combined normal and tangential injection was approximately 50% less than that produced by normal injection alone. An analysis of the change in specific impulse of the scramjet combustor indicated that the best overall performance was produced by 100% normal injection.

Nomenclature

A	=	cross-sectional area
C_D	=	drag coefficient
C_P	=	pressure coefficient
D	=	integrated skin-friction drag
g	=	impulse response
P	=	pressure
t, τ	=	time
u	=	input (drag)
y	=	output (strain)
ϕ	=	equivalence ratio

Subscripts

p, port	=	porthole
s, slot	=	slot
t, tot	=	total

Superscript

$*$	=	property at throat

Introduction

SUPERSONIC combustion ramjets, or scramjets, are expected to allow the economical launch of satellites into low Earth orbit, cut travel times between major cities to a matter of hours, and provide propulsion for high-speed missile applications. Scramjets offer significant performance benefits over other propulsion technologies for atmospheric flight at hypersonic speeds, as a result of their ability to extract the oxygen required for combustion from the atmosphere.[1] However, the large amount of viscous drag present at hypersonic speeds remains one of the major obstacles to the successful development of operational scramjet engines. Depending on the vehicle configuration, the viscous drag can account for up to 40% of the overall drag of a scramjet-powered vehicle.[2] A large component of the total viscous drag can be attributed to supersonic combustors, as a result of the increased density of the flow in this region.

One of the most promising methods of viscous drag reduction is the tangential slot injection of a fluid along a surface, or film cooling. Originally developed as a method of de-icing airplane wings,[3] a tangential slot injection system is "simple to construct, adds thrust to the engine, energises the boundary layer to prevent separation and reduces heating."[4]

Film cooling in low- and high-speed flows has been thoroughly investigated (for example, Goldstein[5]), and experimental measurements have been used to develop expressions for the effectiveness as a function of downstream position divided by slot height x/s and the mass flux ratio of the injectant to the freestream, $\lambda = (\rho u)_j/(\rho u)_\infty$. The use of slot injection for viscous drag reduction, however, is affected by numerous parameters, and the development of empirical correlations has proven extremely difficult. At supersonic or hypersonic speeds, the presence of shock waves, expansion waves, and recompression regions greatly complicates the physical flowfield, as shown in Fig. 1. According to Hefner and Bushnell,[6] the principal independent variables that affect the amount of skin-friction drag reduction are as follows: injectant to freestream velocity ratio, boundary-layer thickness/slot height, state of slot flow (laminar, turbulent, profile shape), slot lip thickness, composition of injectant, local Reynolds number, stream and slot flow turbulence levels, pressure gradients, three dimensionality (discrete holes/slots), and injection angle.

Slot injection reduces viscous drag by modifying the velocity gradient ($\mathrm{d}u/\mathrm{d}y$) at the wall. The velocity gradient is reduced by the injection of low momentum gas, which is then accelerated by the mixing process. The lower the slot flow momentum, the faster the mixing with the external flow, and the faster the slot flow loses its identity.[7] The velocity gradient can also be reduced by the thickening of the boundary layer, which results from the injection of the secondary fluid.[8] Alternatively, the use of lower density gases (for example, hydrogen) can reduce the viscosity of the boundary-layer flow and, therefore, the skin friction in the near wall region.[6] Other factors such as the presence of adverse pressure gradients[9] and the state of the boundary layer[10] can also affect the degree of viscous drag reduction.

However, few studies have examined the effect of combustion, either in the main stream or in the boundary layer, on the viscous drag reduction produced by tangential slot injection. Recent experiments indicate that the presence of boundary-layer combustion can produce a significant reduction in viscous drag.[11,12] The aim of this

Presented as Paper 2005-615 at the AIAA 43rd Aerospace Sciences Meeting and Exhibit, Reno, NV, 10–13 January 2005; received 2 August 2005; revision received 24 August 2005; accepted for publication 19 November 2005.

*Graduate Student, Centre for Hypersonics, Division of Mechanical Engineering. Member AIAA.
†Professorial Research Fellow, Division of Mechanical Engineering, Centre for Hypersonics. Member AIAA.

Table 1 Test flow properties

Property	Nozzle supply	Freestream	Uncertainty, %	Repeatability, %
Pressure	35.8 MPa	78.1 kPa	±14	±4
Temperature	4210 K	1135 K	±12	±4
Enthalpy	5.8 MJ/kg	——	——	——
Density	——	0.240 kg/m^3	±12	±4
Velocity	——	2950 m/s	±5	±2
Mach number	——	4.50	±4	±1

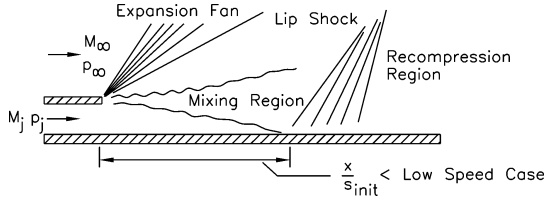

a) Overexpanded slot flow $p_j < p_\infty$

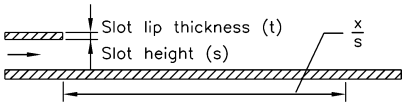

b) Slot geometry

Fig. 1 Slot injection into high-speed flow: a) physical flowfield resulting from overexpanded slot injection into high-speed flow and b) slot geometry parameters (adapted from Hefner and Bushnell[6]).

paper is to investigate the performance of a scramjet combustor fueled by tangential and normal injection, with the aim of reducing viscous drag while maintaining efficient combustion.

Experimental Setup

The experiments were conducted in the T4 free-piston shock tunnel, located at The University of Queensland. An axisymmetric contoured Mach 4 nozzle was used to produce a test flow with a core uniformity of ±5% and a diameter of approximately 100 mm (Ref. 13). Air and nitrogen were used as the primary test gases. The numerical codes, ESTC[14] and NENZF,[15] were used to determine the properties of the flow in the test section (see Table 1). Table 1 shows the average flow properties determined from experiments performed at the nominal test condition. An uncertainty analysis was performed using the method described by Mee.[16] A total of 88 shots, performed at varying equivalence ratios, was used in the analysis. The repeatability of each flow property is also shown in Table 1 and was calculated using a 95% prediction interval.

Stress-Wave Force Balance

A schematic of the single-component stress-wave force balance used in this study is shown in Fig. 2a. This model configuration has been previously used successfully by Tanno et al.[17] and Lentz[18] to make viscous drag and pressure measurements on scramjet combustors.

The supporting stress bar, or sting, is manufactured from brass hollow tubing to minimize non-one-dimensional effects. When used with an aluminum model, as in this study, a brass sting represents the best compromise in terms of low model flexibility, fast response time, and high signal-to-noise ratio.[19] The model was suspended horizontally in the test section by two thin vertical wires to allow it to move freely in the axial (freestream) direction and provide vibration isolation in the horizontal plane. O-rings at the leading and trailing edges of the combustor prevented flow leakage, and six pressure transducers at each end of the combustor measured any residual pressure. The inner and outer shields of the balance, which prevented any external flow disturbances from interfering with the stress bar, were rigidly fixed to the test-section ceiling.

Piezoelectric film (polyvinylidene fluoride) strain gauges[20] were used to measure the strain history of the model during each test. By

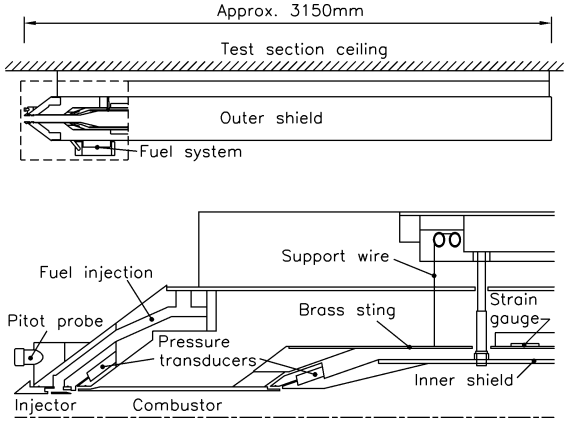

a) Stress-wave force balance

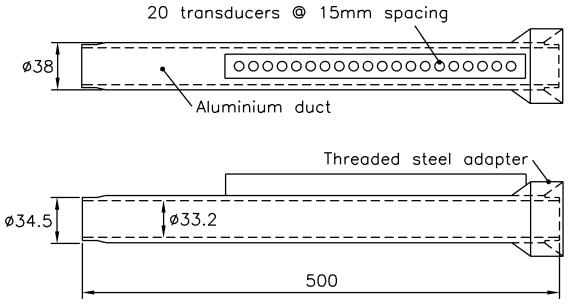

b) Combustor

Fig. 2 Stress-wave force balance and combustor model configuration.

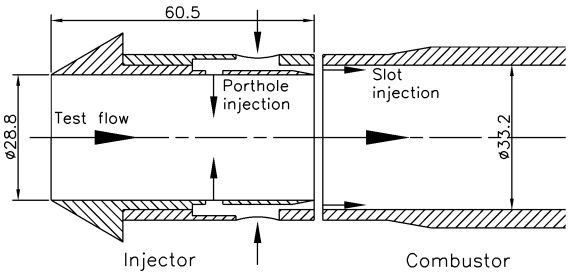

Fig. 3 Fuel-injector design.

modeling the experimental arrangement as a linear system, the total drag can be determined from the convolution integral

$$y(t) = \int_0^t g(t-\tau)u(\tau)\,\mathrm{d}\tau \tag{1}$$

where $u(t)$ is the unknown applied aerodynamic load input, $y(t)$ is the strain output measured at some point on the support structure, and $g(t)$ is the impulse response that describes the relationship between the input and the output. The impulse responses used to process the strain signals were obtained using the pulse-input calibration technique with the impulse response determined by numerical deconvolution.[21] The computer program, HYFORCE,[22] was used to perform the deconvolution process.

Fuel Injectors

A schematic of the general fuel-injector design is shown in Fig. 3. The injectors allowed hydrogen fuel to be injected into the scramjet combustor model tangentially through an annular slot and normally through an array of five portholes. The portholes were 4 mm in diameter and produced sonic injection. The area of the annular slot was varied so that, for a given mass flow rate of fuel through the portholes, each of the four injectors provided a different mass flow rate of fuel along the wall of the scramjet combustor. The geometry of the fuel injectors is summarized in Table 2. Hydrogen fuel was

Table 2 Fuel-injector geometry

Injector	Portholes (A_p, m^2)	Slot throat (A_s^*, m^2)	%Flow (port/slot)
No. 1	6.28×10^{-5}	3.31×10^{-5}	55/45
No. 2	6.28×10^{-5}	5.04×10^{-5}	46/54
No. 3	6.28×10^{-5}	7.90×10^{-5}	38/62
No. 4	6.28×10^{-5}	1.25×10^{-4}	25/75
Lentz	0	6.45×10^{-5}	0/100
Vortex	0	7.90×10^{-5}	0/100

injected from a coiled Ludwieg tube reservoir by a pneumatically actuated solenoid valve triggered by the recoil of the shock tunnel. The fuel equivalence ratio was determined from calibration tests.

Combustor

Two aluminum cylindrical scramjet combustors, 500 mm in length, were used for the experiments, as shown in Fig. 2b. The combustors had an internal diameter of 33.2 mm and an external diameter of 34.5 mm. To reduce the force caused by nonzero pressures at the leading and trailing edges, the combustors were manufactured with a 0.75-mm wall thickness in these regions. One of the combustors was fitted with 20 piezoelectric pressure transducers to measure the wall pressure during the test time. The transducers were recess mounted and spaced at 15-mm intervals along the combustor length. The first transducer was located a distance of 230 mm from the injector entrance.

Results

To account for small variations in the freestream flow conditions during the test time, the average pressure P and viscous drag D were expressed as coefficients

$$C_P = P \big/ 0.5\rho_\infty u_\infty^2 \qquad \text{and} \qquad C_D = D \big/ 0.5\rho_\infty u_\infty^2 A_e$$

where ρ_∞ is the freestream density, u_∞ is the freestream velocity, and A_e is the cross-sectional area of the freestream flow captured by the injector inlet. The dynamic pressure ($0.5\rho_\infty u_\infty^2$) was determined from the results of nozzle calibration tests and the measured nozzle supply pressure using the Rayleigh–pitot relationship.[23] The pressure and drag coefficients were averaged over the test time to produce an average value for each test.

Example pressure and drag coefficients performed with the same test configuration are shown in Fig. 4 for both the fuel-off (pressure, drag) and fuel-on (pressure) cases. Flow arrival is marked by a rapid rise in the measured drag from the zero level. After the flow has established, the test time begins, and the measured drag is expected to remain reasonably steady. However, pressure effects on the semiconductor strain gauges can alter the measured strain and lead to a rise in the measured drag with time. Approximately 3 ms after flow arrival, the model reaches the limit of its travel and makes contact with the inner shielding. This is signified by a sharp drop in the measured drag to values less than zero.

Pressure

The average pressures measured in the combustor for each fuel injector are collated and compared in Fig. 5. The results of Tanno et al.[17] for 100% normal injection are also displayed, as are the results of tests with tangential injection only. In addition, the average pressure coefficient predicted by one-dimensional heat-addition theory is shown.

The results indicate that the presence of normal injection is necessary for combustion to occur. This is confirmed by the results for 100% tangential injection, which are similar in magnitude to the average pressures produced by normal and tangential injection into a nitrogen test flow. The results of tests with various proportions of normal injection indicate that combustion took place when at least 25% of the total mass flow rate was injected normally.

For tests with combined normal and tangential injection, the average combustor pressure was found to be independent of the method

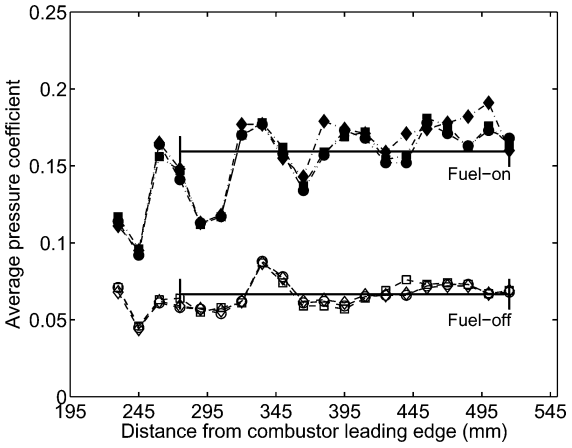

a) Pressure coefficient

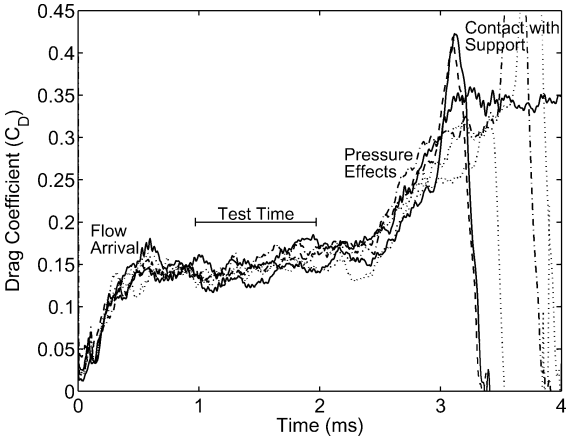

b) Drag coefficient

Fig. 4 Example pressure and drag coefficients.

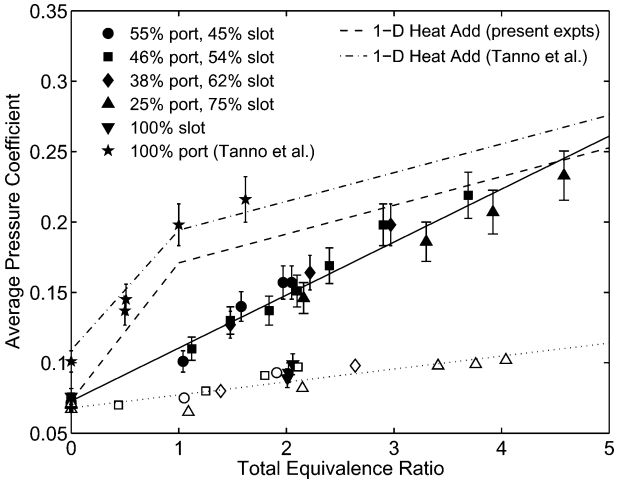

Fig. 5 Effect of total equivalence ratio on average pressure coefficient for injection into air (closed symbols) and nitrogen (open symbols).

in which the fuel was distributed between the porthole and slot injectors within the range of values tested. However, the average pressure coefficient does not approach the levels predicted by theory until a total equivalence ratio of approximately 3. In contrast, the results of Tanno et al. for 100% normal injection result in significantly larger average pressures for a given total equivalence ratio and show good agreement with the corresponding theory. A comparison of the results with previous experiments for 100% normal injection showed that similar combustor pressures were produced when the porthole equivalence ratio was matched. This suggests that only fuel injected

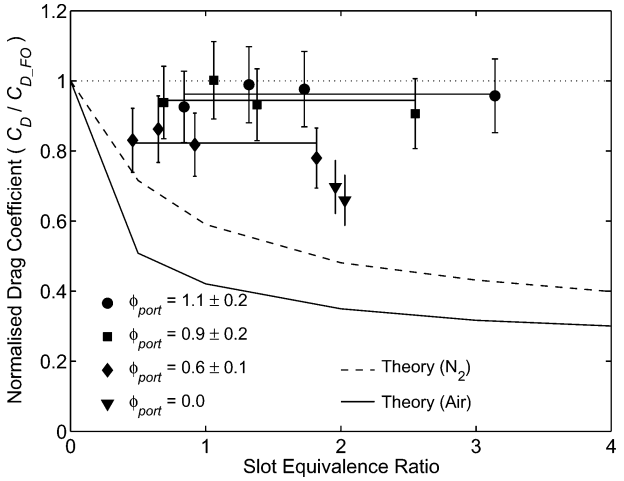

Fig. 6 Effect of slot equivalence ratio on the reduction in viscous drag.

normally combusts when both normal and tangential injection are used.

Viscous Drag

Figure 6 shows the viscous drag measured as a function of slot equivalence ratio. The tests were performed with a test gas of air. The results are presented as the drag coefficient measured with fuel injection normalized by the drag coefficient measured without fuel injection. The results are grouped according to the porthole equivalence ratio.

For the same porthole equivalence ratio, increasing the amount of fuel injected through the slot makes little difference to the drag reduction produced. This indicates that, within the range of total equivalence ratios and injection distributions tested, there is no advantage to be gained by injecting more fuel tangentially along the wall for a given porthole equivalence ratio. When porthole injection is not present, as shown by the results for tangential slot injection only, the hydrogen film produced by slot injection remains intact, and greater reductions in viscous drag are realized. This trend is also predicted by the modified van Driest II theory of Stalker,[24] which considers the effects of boundary layer combustion.

As the porthole equivalence ratio is increased, the viscous drag measured on the combustor increases for a given slot equivalence ratio. The increase in the porthole equivalence ratio creates stronger disturbances in the flow and reduces the effect of tangential injection on the viscous drag, as shown in Fig. 7a. Similar results are obtained for injection into both air and nitrogen test flows, indicating that the presence of combustion does not significantly affect any reduction in the viscous drag.

To confirm the effect of normal injection on the reduction in viscous drag, tests were conducted with an injector that had vortex generators in place of the portholes for normal injection. The vortex generators were triangular in shape and were designed to generate pairs of counter-rotating vortices similar to those produced by the normal injection of fuel. The results are shown in Fig. 7b. The trend in viscous drag is similar to that observed with changes in the porthole equivalence ratio—as the height of the vortex generators is increased, and larger counter-rotating vortices are produced, the level of viscous drag increases towards the fuel-off value. This is an important result as it confirms that it is the flow disturbances associated with normal injection and not the presence of combustion itself that affects the reduction in viscous drag produced by tangential slot injection.

Specific Impulse

A representative scramjet vehicle that might employ a combustor design similar to that used in the present study is shown in Fig. 8. For the purposes of the analysis presented here, the inlet and exit areas of the scramjet engine are fixed at 0.01 m^2. The vehicle would have a simulated flight Mach number of approximately 8.25, assuming

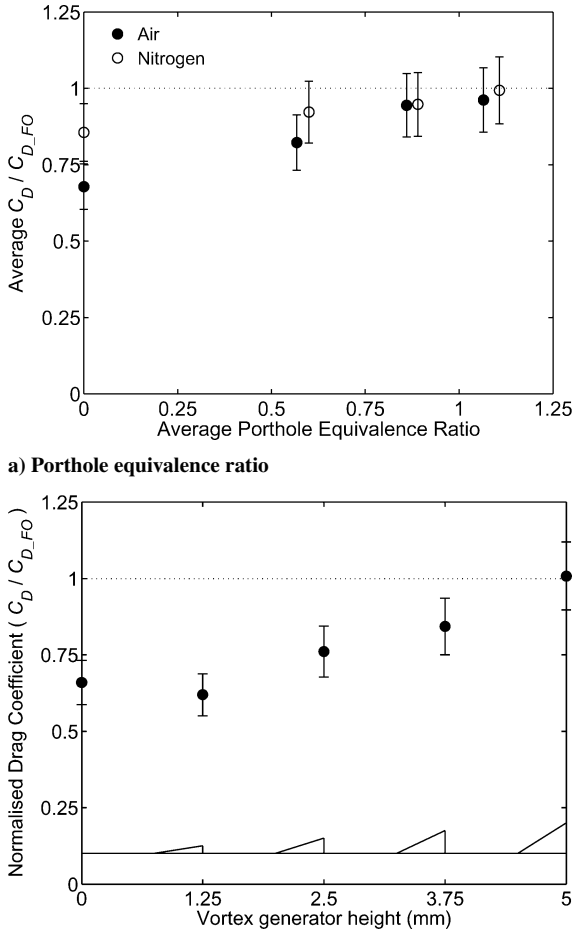

a) Porthole equivalence ratio

b) Vortex generators

Fig. 7 Reduction in viscous drag with a) porthole equivalence ratio and b) vortex generator height.

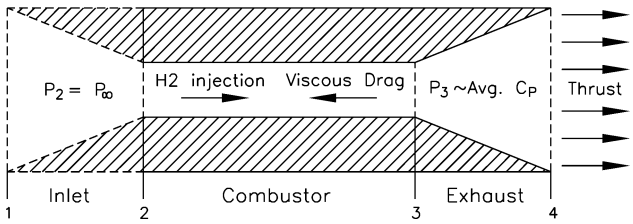

Fig. 8 Representative scramjet vehicle.

that the flow is isentropically compressed from the inlet (station 1) to the combustor entrance (station 2). The corresponding simulated flight altitude is approximately 27 km.

As only a scramjet combustor is being evaluated in this study, it is appropriate to consider the change in the specific impulse that occurs with fuel injection rather than the overall specific impulse. The inlet performance is unaffected by the combustor design and is excluded from the analysis. There are three forces related to the scramjet combustor design shown in Fig. 8 that affect the change in specific impulse: the viscous drag D, the thrust resulting from tangential fuel injection F_I, and the thrust produced by the expansion of the combustor exit flow F_P.

The change in specific impulse as a function of total equivalence ratio for various proportions of normal and tangential injection is shown in Fig. 9. All of the tests were performed with a 500-mm combustor at test condition A using air as the test gas. Data are also shown for 100% tangential injection and 100% normal injection. Tanno et al.[17] indicated that the viscous drag was not significantly affected by the normal injection of fuel. Therefore, for the purposes of analysis the viscous drag in the case of 100% normal injection

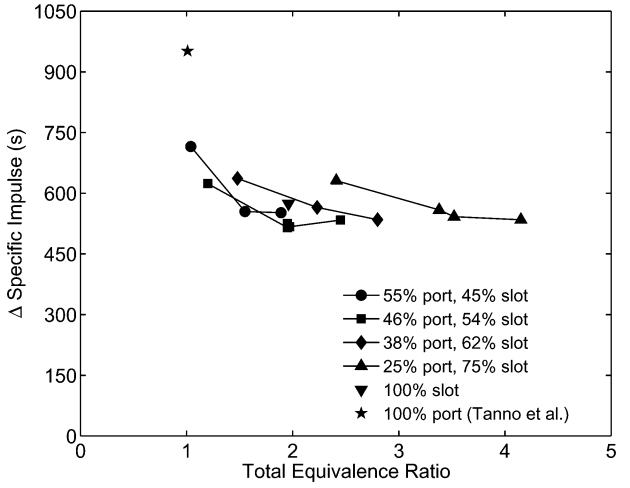

Fig. 9 Change in specific impulse for various proportions of normal and tangential injection.

was assumed to be equal to the viscous drag measured without fuel injection in the present study.

The most significant result is that the greatest increase in the specific impulse is produced by 100% normal injection. In comparison, the greatest increase in the specific impulse for combined normal and tangential injection is approximately 20% less. In other words, the change in the specific impulse that results from the viscous drag reduction produced by tangential injection is less than the change in the specific impulse that would result from the combustor pressure rise produced by the normal injection of that fuel. Therefore, for the current experimental configuration the results indicate that the best overall performance is achieved using normal injection only.

For combined normal and tangential injection, the greatest increase in specific impulse for each injection distribution occurs at the lowest value of the total equivalence ratio tested. In addition, with the exception of the no. 1 injector, the minimum and maximum values of the change in the specific impulse are approximately the same for all injectors. This indicates that the change in specific impulse is almost independent of the fuel-injection distribution within the range of values tested.

Conclusions

The average pressure and viscous drag of a 500-mm-long cylindrical scramjet combustor with combined normal and tangential injection were measured at a range of equivalence ratios and the resulting change in the specific impulse calculated. The results indicated that the presence of normal injection was necessary for combustion to occur. However, the average pressure produced by normal and tangential injection was approximately half that produced by normal injection alone. As a result, an analysis of the change in specific impulse showed that the best performance was obtained from 100% normal injection. For combined tangential and normal injection, the overall performance of the scramjet combustor decreased as a greater percentage of the fuel was injected tangentially, and the largest increase in specific impulse was obtained with the no. 1 injector, which had the largest proportion of normal injection.

Larger reductions in viscous drag were observed at low values of the porthole equivalence ratio, and it was found that the presence of normal injection disrupted the layer of fuel injected tangentially and led to an increase in the viscous drag. Therefore, at this particular test condition there might be other injection configurations where better results are achievable. For example, if breaking up of the wall boundary layer can be prevented, tangential injection may be effective in reducing viscous drag and improving overall performance. There was little change in the viscous drag as the slot equivalence ratio was increased.

Acknowledgments

The authors would like to acknowledge the financial support provided for this research by the Australian Postgraduate Awards Scheme and The University of Queensland. Thanks are also due to David Mee of The University of Queensland for his many helpful suggestions and technical comments during the preparation of this paper.

References

[1]Kors, D., "Design Considerations for Combined Air Breathing-Rocket Propulsion Systems," AIAA Paper 90-5216, Oct. 1990.

[2]Lewis, D. P., and Schetz, J. A., "Tangential Injection from Overlaid Slots into a Supersonic Stream," *Journal of Propulsion and Power*, Vol. 13, No. 1, 1997, pp. 59–63.

[3]Goldstein, R. J., Eckert, E. R. G., Tsou, F. K., and Haji-Sheikh, A., "Film Cooling with Air and Helium Injection Through a Rearward-Facing Slot into a Supersonic Air Flow," *AIAA Journal*, Vol. 4, No. 6, 1966, pp. 981–985.

[4]Juhany, K. A., and Hunt, M. L., "Flowfield Measurements in Supersonic Film Cooling Including the Effect of Shock-Wave Interaction," *AIAA Journal*, Vol. 32, No. 3, 1994, pp. 578–585.

[5]Goldstein, R. J., "Film Cooling," *Advances in Heat Transfer*, Vol. 7, 1971, pp. 321–379.

[6]Hefner, J. N., and Bushnell, D. M., "Viscous Drag Reduction via Surface Mass Injection," *Viscous Drag Reduction in Boundary Layers*, edited by J. N. Hefner and D. M. Bushnell, Progress in Astronautics and Aeronautics, AIAA, Washington, DC, 1990, pp. 457–476.

[7]Srokowski, A. J., Howard, F. G., and Feller, W. V., "Direct Measurements at Mach 6 of Turbulent Skin-Friction Reduction by Injection from Single and Multiple Flush Slots," AIAA Paper 76-178, Jan. 1976.

[8]Fischer, M. C., and Ash, R. L., "A General Review of Concepts for Reducing Skin Friction, Including Recommendations for Future Studies," NASA TM X-2894, Nov. 1973.

[9]Hefner, J. N., "Effect of Geometry Modifications on Effectiveness of Slot Injection in Hypersonic Flow," *AIAA Journal*, Vol. 14, No. 6, 1976, pp. 817, 818.

[10]Richards, B. E., and Stollery, J. L., "Laminar Film Cooling Experiments in Hypersonic Flow," *Journal of Aircraft*, Vol. 16, No. 3, 1979, pp. 177–181.

[11]Goyne, C. P., Stalker, R. J., Paull, A., and Brescianini, C. P., "Hypervelocity Skin-Friction Reduction by Boundary-Layer Combustion of Hydrogen," *Journal of Spacecraft and Rockets*, Vol. 37, No. 6, 2000, pp. 740–746.

[12]Suraweera, M., Mee, D., and Stalker, R., "Skin Friction Reduction in Hypersonic Turbulent Flow by Boundary Layer Combustion," AIAA Paper 2005-613, Jan. 2005.

[13]Jacobs, P. A., and Stalker, R. J., "Mach 4 and Mach 8 Axisymmetric Nozzles for a High-Enthalpy Shock Tunnel," *Aeronautical Journal*, Vol. 95, No. 933, 1991, pp. 324–334.

[14]McIntosh, M. K.,"Computer Program for the Numerical Calculation of Frozen and Equilibrium Conditions in Shock Tunnels," Dept. of Supply, Australian Defence Scientific Service, Weapons Research Establishment, Technical Note CPD 169, Salisbury, Australia, April 1970.

[15]Lordi, J. A., Mates, R. E., and Moselle, J. R., "Computer Program for the Numerical Simulation of Non-Equilibrium Expansions of Reacting Gas Mixtures," NASA CR-472, May 1966.

[16]Mee, D. J., "Uncertainty Analysis of Conditions in the Test Section of the T4 Shock Tunnel," Dept. of Mechanical Engineering, Rept. 4/93, Univ. of Queensland, Brisbane, 1993.

[17]Tanno, H., Paull, A., and Stalker, R. J., "Skin-Friction Measurements in a Supersonic Combustor with Crossflow Fuel Injection," *Journal of Propulsion and Power*, Vol. 17, No. 6, 2001, pp. 1333–1338.

[18]Lentz, S., "Preliminary Investigation of Viscous Drag Reduction on a Scramjet Combustion Chamber," Div. of Mechanical Engineering, Univ. of Queensland, Unpublished Report, Brisbane, Australia, June 1998.

[19]Sanderson, S. R., and Simmons, J. M., "Drag Balance for Hypervelocity Impulse Facilities," *AIAA Journal*, Vol. 29, No. 12, 1991, pp. 2185–2191.

[20]Smith, A. L., and Mee, D. J., "Dynamic Strain Measurment Using Piezoelectric Polymer Film," *Journal of Strain Analysis*, Vol. 31, No. 6, 1996, pp. 463–465.

[21]Mee, D. J., "Dynamic Calibration of Force Balances for Hypersonic Impulse Facilities," *Shock Waves*, Vol. 12, No. 6, 2003, pp. 443–455.

[22]Mee, D. J., "HYFORCE Computer Program for Signal Recovery on Stress Wave Force Balances," Dept. of Mechanical Engineering, Univ. of Queensland, Brisbane, Dec. 2000.

[23]"Equations, Tables and Charts for Compressible Flow," NACA Report 1135, 1953.

[24]Stalker, R. J., "Light Launch Vehicles and Control of Skin Friction Losses," Paper AIAC2003-053, *Proceedings of the 10th Australian International Aerospace Congress*, edited by D. J. Mee, Engineers Australia, 2003.